Nb 2 O 2 F 3 : A Reduced Niobium (III/IV) Oxyfluoride with a Complex Structural, Magnetic, and Electronic Phase Transition

ARTICLE *in* JOURNAL OF THE AMERICAN CHEMICAL SOCIETY · JANUARY 2015

Impact Factor: 12.11 · DOI: 10.1021/ja511745q

JACS
JOURNAL OF THE AMERICAN CHEMICAL SOCIETY
Communication
pubs.acs.org/JACS

$Nb_2O_2F_3$: A Reduced Niobium (III/IV) Oxyfluoride with a Complex Structural, Magnetic, and Electronic Phase Transition

T. Thao Tran,[†,§] Melissa Gooch,[‡,§] Bernd Lorenz,[‡,§] Alexander P. Litvinchuk,[‡,§] Maurice G. Sorolla, II,[†,§] Jakoah Brgoch,[†,§] Paul C. W. Chu,[‡,§,∥] and Arnold M. Guloy*[,†,§]

[†]Department of Chemistry, [‡]Department of Physics, and [§]Texas Center for Superconductivity, University of Houston, Houston, Texas 77204, United States

[∥]Lawrence Berkeley National Laboratory, Berkeley, California 94720, United States

Supporting Information

ABSTRACT: A new niobium oxyfluoride, $Nb_2O_2F_3$, synthesized through the reaction of Nb, SnO, and SnF_2 in Sn flux, within welded Nb containers, crystallizes in a monoclinic structure (space group: $I2/a$; a = 5.7048(1)Å, b = 5.1610(1)Å, c = 12.2285(2)Å, β = 95.751(1)°). It features $[Nb_2X_{10}]$ units (X = O, F), with short (2.5739(1) Å) Nb−Nb bonds, that are linked through shared O/F vertices to form a 3D structure configurationally isotypic to ζ-Nb_2O_5. $Nb_2O_2F_3$ undergoes a structural transition at ∼90 K to a triclinic structure (space group: $P\bar{1}$; a = 5.1791(5)Å, b = 5.7043(6)Å, c = 6.8911(7)Å, α = 108.669(3)°, β = 109.922(2)°, γ = 90.332(3)°). The transition is described as a disproportionation or charge ordering of $[Nb_2]^{7+}$ dimers: $(2[Nb_2]^{7+} \rightarrow [Nb_2]^{6+} + [Nb_2]^{8+})$, resulting in doubly (2.5000(9) Å) and singly bonded (2.6560(9) Å) Nb_2 dimers. The structural transition is accompanied by an unusual field-independent "spin-gap-like" magnetic transition.

The design and synthesis of new materials with desired and tunable properties continues to be a major goal of synthetic solid-state chemists. One such class of materials are strongly correlated electron systems which exhibit a range of unusual physical phenomena, such as superconductivity, charge density wave, spin density wave, metal−insulator transitions, and low-dimensional electronic and magnetic properties.[1−3] Strongly correlated electronic materials provide a foundation for a new understanding of the physics and chemical bonding of the solid state.[4,5] Reduced early transition-metal oxides and halides have been an intense area of chemical research for many decades, owing to the abundance of novel structures and compounds they exhibit, and hence offer a fertile area for exploratory research for new strongly correlated materials.

On the basis of known intrinsic physical behaviors, compounds of niobium in low oxidation states have been of significant interest.[6] Reduced niobium halides and chalcogenides form a wealth of metal−metal bonded cluster compounds.[7,8] In contrast, the number of reduced Nb oxides and fluorides is relatively moderate, and the synthesis of reduced niobium oxyfluorides remains a challenge. Yet, interesting properties have been observed in some low-valent oxoniobates: $Nb_{12}O_{29}$ with an average Nb valence of 4.83 was reported to be a metallic antiferromagnet (T_N = 12 K);[9] $BaNbO_{3-x}$ was reported to be superconducting, with $T_c \sim 20$ K;[10] Li_xNbO_2, with $0.45 < x < 0.80$, was reported to be metallic and superconducting at temperatures below 5 K.[11]

The chemistry of niobium oxyfluorides is primarily dominated by the pentavalent state Nb(V).[12] Synthetic routes to Nb oxyfluorides (solid-state and hydrothermal reactions), using appropriate starting materials, are usually performed at high temperatures and/or under highly oxidizing (acidic) conditions that often result with Nb in its highest oxidation state.[7] Successful synthesis of reduced Nb oxyfluorides has so far been limited to $NaNb_3O_5F$ and $ANbO_2F$ (A = Li, Na, or K).[13,14] It is also noted that cubic NbF_3 (ReO_3-type) may actually contain and stabilized by oxygen.[15,16] Herein we report the synthesis and characterization of a reduced mixed-valent Nb(III/IV) oxyfluoride, $Nb_2O_2F_3$, including its crystal structure, physical properties (transport, magnetism, vibrational spectra, and heat capacity), and chemical bonding.

The title compound was synthesized from the reaction of Nb, SnF_2, and SnO in Sn flux within welded Nb containers, enclosed in evacuated fused silica jackets. The synthesis procedure is a modification of the reported synthesis of reduced niobium fluorides.[17] Shiny black crystals obtained from the flux reactions were subsequently determined to be $Nb_2O_2F_3$ by single crystal and powder X-ray diffraction and confirmed by chemical analysis. Phase pure stoichiometric samples were subsequently prepared for property measurements. All experimental manipulations were performed under inert conditions within a purified Ar-atmosphere glovebox with total H_2O and O_2 level of <0.1 ppm. Details of the experimental procedures, results of the chemical analyses and other measurements, X-ray crystallographic data and refinement, and other and relevant crystallographic tables are given in the Supporting Information.

The monoclinic ($I2/a$) crystal structure of $Nb_2O_2F_3$ in Figure 1a features $[Nb_2O_4F_6]$ dimeric units with short Nb−Nb bonds of 2.5739(1) Å. Since differentiation between O and F atoms cannot be confirmed by X-ray diffraction (and for simplicity) the assignment Nb_2X_5 (X = O, F) will be used in the structural description. The dimers can be described as $[Nb_2(\mu_2\text{-}X)_2X_8]$ units consisting of two distorted NbX_6 octahedra condensed through shared edges. Neighboring $[Nb_2(\mu_2\text{-}X)_2X_8]$

Received: November 25, 2014
Published: December 31, 2014

DOI: 10.1021/ja511745q
J. Am. Chem. Soc. 2015, 137, 636−639

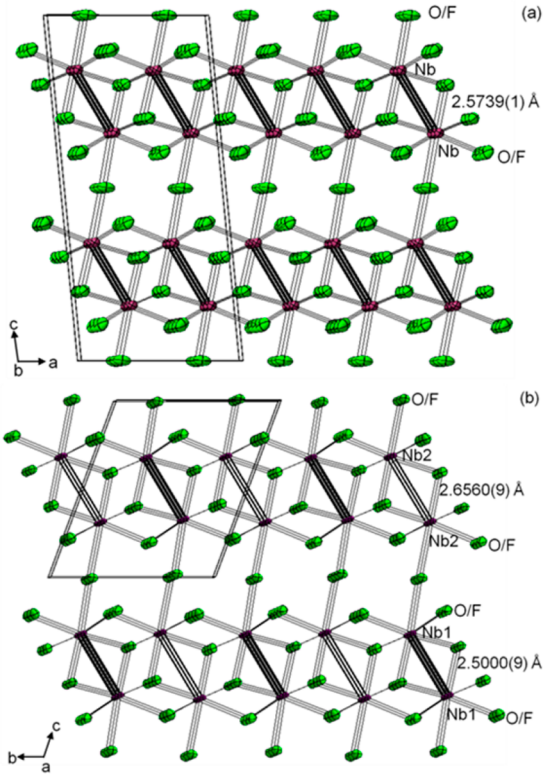

Figure 1. ORTEP representation of the crystal structures of (a) monoclinic (M)-$Nb_2O_2F_3$ and (b) triclinic (T)-$Nb_2O_2F_3$. Ellipsoids are drawn at 90% probability.

units are linked through shared vertices of eight X atoms to form $[\{Nb_2(\mu_2\text{-}X)_{2\times2/3}X_{2\times1/3}X_{6/2}\}_\infty]$ slabs along the $a-b$ plane. The slabs are then linked through the two other bridging ligands (X) along the c-axis to form a 3D Nb_2X_5 network, as shown in Figure 1a. The Nb−X distances in the Nb_2X_{10} dimer units, range from 1.9586(8) to 2.1158(7) Å. The monoclinic structure is configurationally isotypic to ζ-Nb_2O_5,[18] albeit the shortest Nb−Nb distances (3.404(5) Å) in ζ-Nb_2O_5 are nonbonding. Hence, a formal topochemical relationship exists between $Nb_2O_2F_3$ and ζ-Nb_2O_5, wherein F substitution of O in ζ-Nb_2O_5 results in the chemical reduction of Nb and formation of Nb−Nb bonds.

The magnetic susceptibility of $Nb_2O_2F_3$ (in Figure 2a) increases upon cooling below room temperature and shows a precipitous drop below 90 K, indicating a phase transition that quenches the magnetic moment. A large thermal hysteresis of the cooling and heating data is observed, indicating a first-order nature of the phase transition. Quenching of the magnetic moment at the transition suggests a spin-gap formation, often observed in a spin-Peierls system, with the pairing of two spins forming a singlet state with no spin momentum.[19,20] To clarify whether the transition is driven by magnetic interactions as in spin-Peierls systems, the transition was further investigated in the vicinity of the critical temperature, as a function of magnetic field (up to 5 T). No change in the transition temperature or the width of the thermal hysteresis was observed (Figure S4), indicating that a magnetic origin of the phase transition is unlikely.

Above the critical temperature (T > 100 K) the susceptibility fits Curie−Weiss law, with a small diamagnetic contribution ($\chi_0 = -5 \times 10^{-4}$ emu/mol) ascribed to the paired 4d electrons in the Nb−Nb bond. The inverse susceptibility, $(\chi-\chi_0)^{-1}$, also

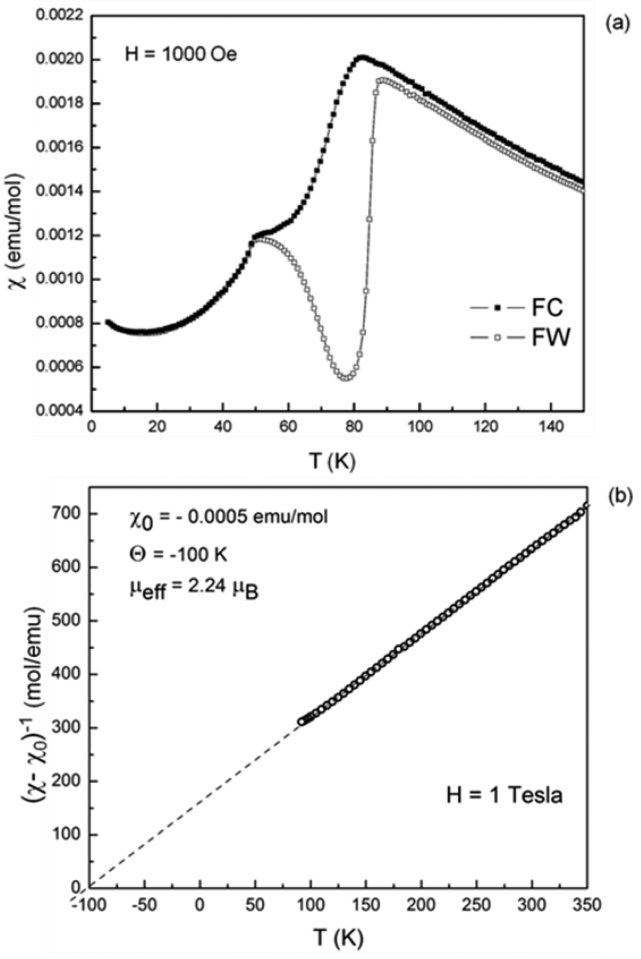

Figure 2. (a) Magnetic susceptibility (χ) of $Nb_2O_2F_3$ upon field cooling (FC) and field warming (FW), T = 2−150 K, H = 1000 Oe and (b) the reciprocal of magnetic susceptibility ($\chi-\chi_0$) of $Nb_2O_2F_3$ as a function of temperature (T > 90 K), H = 1 T.

changes linearly with temperature (Figure 2b) above the phase transition, with the Weiss temperature (Θ = −100 K) indicating antiferromagnetic exchange interactions between the Nb_2 dimer spins. The effective magnetic moment, μ_{eff} = 2.24 μ_B, (per Nb_2 dimer) is consistent with S = 1/2 and a $[Nb-Nb]^{7+}O_2F_3$ assignment with Nb−Nb bond order of 1.5; having unpaired electrons at the Nb π-bonding orbitals. The slightly larger value of μ_{eff} to the spin only value of 1.74 can be attributed to an incompletely quenched orbital moment. The thermodynamic signatures of the two anomalies of χ observed at ∼50 and ∼90 K were confirmed by heat capacity (C_p) measurements (Figure S5). In between the transition temperatures, C_p follows the normal temperature dependence, although the magnetization reveals large thermal hysteresis effects. The observed temperature dependence of the magnetization suggests possible coexistence of competing magnetic states, and further investigations on the phase transitions, particularly at 50 K, are needed.

Electrical transport measurements on $Nb_2O_2F_3$ indicate a semiconducting temperature dependence of the resistivity (in Figure 3). The resistivity (ρ) increases sharply reaching a magnitude of nearly giga-ohms-cm near the 90 K phase transition. At the critical temperature, ρ appears to show a maximum, and begins to drop at lower temperatures.

DOI: 10.1021/ja511745q
J. Am. Chem. Soc. 2015, 137, 636−639

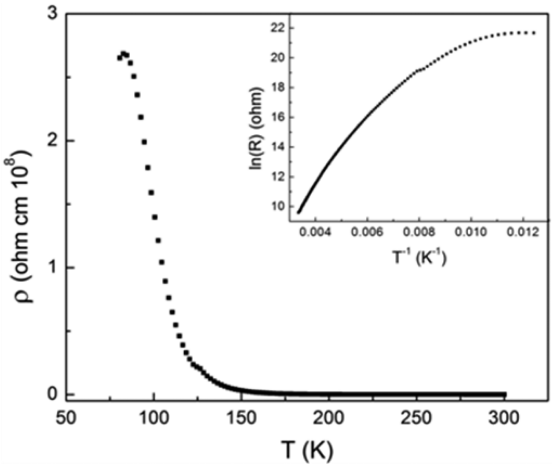

Figure 3. Plot of resistivity (ρ) of $Nb_2O_2F_3$ as a function of temperature (T = 80−300 K). Inset: plot of ln(R) vs 1/T.

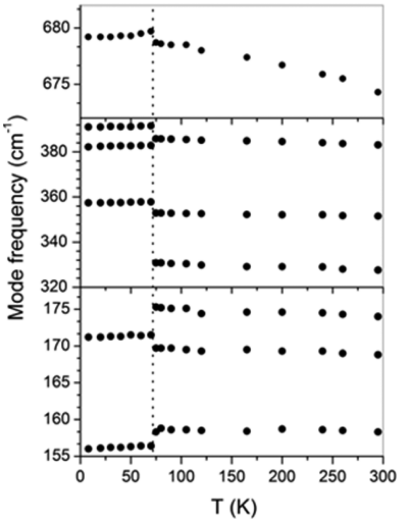

Figure 4. Temperature dependence (T = 8−295 K) of selected Raman-active mode frequencies of $Nb_2O_2F_3$. The phase transition at 90 K is indicated by a dashed line.

However, transport measurements could not be extended to below 80 K since contact resistance increased and any unguarded measurement becomes questionable in this range. The inset in Figure 3 shows that a simple thermally activated conduction process cannot describe the data very well (the plot of ln(R) vs 1/T is expected to be linear). Thus, $Nb_2O_2F_3$ is not a simple semiconductor and suggests a more complex transport mechanism, like variable range hopping behavior wherein electronic correlations and/or disorder induced by oxygen−fluorine disorder play important roles.[21]

Single crystal structure determination, performed at 83 K, revealed the structural nature of the phase transition at 90 K. A structural transition from a monoclinic ($I2/a$) to triclinic lattice ($P\bar{1}$) is observed, represented by the loss of I-centering in the monoclinic lattice. The symmetry reduction is manifested by the emergence of two nonequivalent Nb_2X_{10} dimers with dissimilar Nb−Nb bond lengths in the triclinic structure (in Figure 1b). One Nb_2X_{10} unit has shorter (2.5000(9) Å), and the other has longer (2.6560(9) Å) Nb−Nb bond lengths. The structural transition can be viewed as a charge ordering (CDW) or disproportionation into mixed-valent dimer states: $2[Nb_2]^{7+} \rightarrow [Nb_2]^{6+} + [Nb_2]^{8+}$, wherein $[Nb_2]^{6+}$ and $[Nb_2]^{8+}$ dimers have double and single bonds, respectively. Furthermore, the spin-gap behavior can be attributed to a transition from a Mott insulating paramagnetic state (M-$Nb_2O_2F_3$) with S = 1/2, to a mixed-valent or CDW state (T-$Nb_2O_2F_3$) with S = 0.

The structural phase transition at 90 K is confirmed by Raman scattering measurements, where the mode frequencies as a function of temperature (8−295 K) were observed to remarkably change at temperatures below 90 K (Figure S6). The observed number of Raman-active modes and their position agree well with calculated values. In lowering the temperature to ∼90 K no changes are observed in the scattering spectra apart from normal (some small hardening) shifts of lines due to lattice anharmonicity (Figure 4). However, drastic changes occur upon cooling below the transition temperature. Most of the scattering lines are shifted in frequency by as much as 10 cm^{-1}. However, the total number of observed lines remains the same, as the number of atoms within primitive cells (I-centered monoclinic and triclinic) is unchanged. No changes in the Raman spectra were observed upon cooling below 80 K, indicating the magnetic transition observed at ∼50 K, as shown by the heat capacity measurements, does not involve a structural transformation.

The electronic structure and metal−metal bonding of molecular M_2X_{10} units as in $Nb_2O_2F_3$ have been well studied.[22,23] A simple molecular orbital (MO) analyses provides a useful starting point in understanding the structural/electronic behavior of the title compound. Metal−metal bonding interactions arise from the orbital mixing of the t_{2g}-derived 4d orbitals of Nb atoms forming six hybrid MOs, listed in increasing energy: σ, π, δ, δ^*, π^*, σ^*; (e_g-derived Nb orbitals are involved in Nb−O/F interactions). Allowing for Nb_2^{7+} (d^1−d^2) electron assignment in the Nb_2 dimer leads to an electron configuration: σ^2, π^1; with Nb−Nb bond order of 1.5. It is noted that the observed Nb−Nb distance in $Nb_2O_2F_3$ is shorter than the reported Nb−Nb triple bond distance (2.614 Å) in $NaNb_3O_5F$,[13] nevertheless Nb−Nb bonds have also been reported to be insensitive to bond multiplicity.[24] Continuing the MO arguments to the extended solid, bands around the Fermi level are expected to be t_{2g}-derived Nb_2 states. The expected band filling corresponds to a metallic half-filled π-band which gives rise to instability with respect to possible magnetic ordering, bond formation, and/or charge ordering.[25,26]

The semiconducting and paramagnetic behavior of $Nb_2O_2F_3$ above 90 K suggests strong correlations akin to Mott insulators. Density functional theory confirms the results of classical MO analysis. Using the Vienna ab initio simulation package,[27] the spin-polarized electronic structure was calculated for the monoclinic and triclinic structures. Exchange and correlation was described by the screened hybrid functional, HSE06[28] with the calculations employing γ-centered k-mesh grids of 6 × 6 × 4 and 6 × 6 × 6 for the monoclinic and triclinic structures, respectively, and a cutoff energy for the plane-wave basis set of 500 eV for both structures. The monoclinic structure (Figure 5a) is a semiconductor with a calculated band gap of ∼1 eV. The density of states (DOS) near the Fermi level are comprised of exclusively Nb d-states. Bands below E_F arise from fully filled π- and σ-interactions of the Nb_2^{7+} ions, in agreement with the MO theory and consistent with Nb−Nb dimer formation. Surprisingly, the transformation to the triclinic structure on cooling leads to a unique electronic rearrangement, most

DOI: 10.1021/ja511745q
J. Am. Chem. Soc. 2015, 137, 636−639

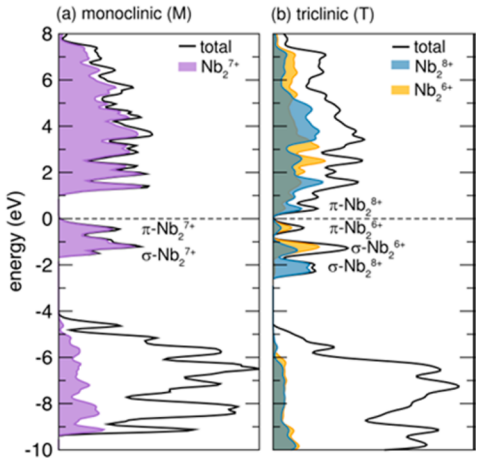

Figure 5. DOS of (a) (M)-$Nb_2O_2F_3$ with the partial DOS for the Nb_2^{7+} dimers and (b) (T)-$Nb_2O_2F_3$ with the partial DOS for the Nb_2^{8+} and Nb_2^{6+} dimers shown. The respective Fermi levels (E_F) are set at 0 eV.

notably a loss of the band gap (Figure 5b). As a result, $Nb_2O_2F_3$ is predicted to undergo a semiconductor-to-metal transition coupled with the structural distortion, and the triclinic phase is calculated to exhibit a deep, nonzero pseudogap at E_F indicating poor metallic character. The bands below the pseudogap are associated with the shorter Nb_2^{6+}, corresponding to a fully filled σ- and π-interactions yielding an electron configuration of $\sigma^2\,\pi^2$ or Nb═Nb double bonds. In contrast, the interactions for the longer Nb_2^{8+} dimers show σ-interactions fully filled below E_F, while corresponding π-interactions are unoccupied. The result is an electron configuration of σ^2 or Nb−Nb single bonds.

$Nb_2O_2F_3$ represents a unique example of a reduced niobium oxyfluoride derived from ligand (F/O) substitution in a simple binary oxide, ζ-Nb_2O_5. It undergoes an unusual "spin-gap" formation (T < 90 K) arising from the disproportionation of paramagnetic metal−metal bonded Nb_2 dimers. A similar "spin-gap" behavior associated with metal bond formation has been reported for a complex ruthenate, $Ba_3NaRu_2O_9$.[29,30] The "spin-gap" transition in $Nb_2O_2F_3$ is theoretically predicted to be accompanied by the loss of a band gap. Detailed description and a more systematic analysis of the low-temperature transport and magnetic behavior of $Nb_2O_2F_3$ will be presented in a separate report.

■ ASSOCIATED CONTENT

Ⓢ Supporting Information

Additional details and crystallographic data. This material is available free of charge via the Internet at http://pubs.acs.org

■ AUTHOR INFORMATION

Corresponding Author

aguloy@uh.edu

Notes

The authors declare no competing financial interest.

■ ACKNOWLEDGMENTS

This work was supported in part by the R. A. Welch Foundation (E-1297), the State of Texas through the Texas Center for Superconductivity, and the US AFOSR. We thank Dr. J. D. Korp for assistance in collecting low-temperature X-ray diffraction data. T.T.T. acknowledges Prof. P. S. Halasyamani.

■ REFERENCES

(1) Simon, A. *Angew. Chem., Int. Ed. Engl.* **1997**, *36*, 1789.
(2) Gabovich, A. M.; Voitenko, A. I.; Ausloos, M. *Phys. Rep.* **2002**, *367*, 583.
(3) Morosan, E.; Natelson, D.; Nevidomskyy, A. H.; Si, Q. *Adv. Mater.* **2012**, *24*, 4896.
(4) von Lohneysen, H.; Rosch, A.; Vojta, M.; Wolfle, P. *Rev. Mod. Phys.* **2007**, *79*, 1015.
(5) Canadell, E.; Whangbo, M. H. *Chem. Rev.* **1991**, *91*, 965.
(6) Köhler, J.; Svensson, G.; Simon, A. *Angew. Chem., Int. Ed. Engl.* **1992**, *31*, 1421.
(7) Simon, A. *Angew. Chem., Int. Ed. Engl.* **1981**, *20*, 1.
(8) Schäfer, H.; Schnering, H. G. *Angew. Chem.* **1964**, *76*, 833.
(9) Cava, R. J.; Batlogg, B.; Krajewski, J. J.; Gammel, P.; Poulsen, H. F.; Peck, W. F., Jr.; Rupp, L. W., Jr. *Nature* **1991**, *350*, 598.
(10) Strukova, G. K.; Kedrov, V.; Zverev, V.; Khasanov, S.; Ovchinnikov, I.; Batov, I. E.; Gasparov, V. A. *Physica C* **1997**, *291*, 207.
(11) Geselbracht, M. J.; Richardson, T. J.; Stacy, A. M. *Nature* **1990**, *345*, 324.
(12) (a) Nieder-Vahrenholz, H. G.; Schäfer, H. Z. *Anorg. Allg. Chem.* **1987**, *544*, 122. (b) Cordier, S.; Roisnel, T.; Poulain, M. J. *Solid State Chem.* **2004**, *177*, 3119. (c) Guelin, J.; Ravez, J.; Hagenmuller, P. *J. Less-Common Met.* **1988**, *137*, 75. (d) Wadsley, A.; Andersson, S. *Perspect. Struct. Chem.* **1970**, *3*, 1.
(13) Köhler, J.; Simon, A. *Angew. Chem., Int. Ed. Engl.* **1986**, *25*, 996.
(14) Ruedorff, W.; Krug, D. Z. *Anorg. Allg. Chem.* **1964**, *329*, 211.
(15) Schäfer, H.; Schnering, H. G.; Niehues, K. J.; Nieder-Vahrenholz, H. G. *J. Less-Common Met.* **1965**, *9*, 95.
(16) Delobbe, V.; Chassaing, J.; Bizot, D. *Rev. Chim. Miner.* **1985**, *22*, 784.
(17) Gortsema, F. P.; Didchenko, R. *Inorg. Chem.* **1965**, *4*, 182.
(18) Ercit, T. S. *Mineral. Petrol.* **1991**, *43*, 217.
(19) Khomskii, D. I. *Prog. Theor. Phys. Suppl.* **2005**, *159*, 319.
(20) Voit, J. *Rep. Prog. Phys.* **1995**, *58*, 977.
(21) Mott, N. F. *Philos. Mag.* **1969**, *19*, 835.
(22) Goddard, R. J.; Hoffmann, R.; Jemmis, E. D. *J. Am. Chem. Soc.* **1980**, *102*, 7667.
(23) Cotton, F. A.; Diebold, M. P.; O'Connor, C.; Powell, G. L. *J. Am. Chem. Soc.* **1985**, *107*, 7438.
(24) Tayebani, M.; Feghali, K.; Gambarotta, S.; Yap, G. P. A. *Inorg. Chem.* **2001**, *40*, 1399.
(25) Whangbo, M. H. *Acc. Chem. Res.* **1983**, *16*, 95.
(26) Austin, I. G.; Mott, N. F. *Science* **1970**, *168*, 71.
(27) (a) Kresse, G.; Hafner, J. *Phys. Rev. B* **1993**, *47*, 558. (b) Kresse, G.; Furthmüller, J. *J. Comput. Mater. Sci.* **1996**, *6*, 15. (c) Kresse, G.; Joubert, D. *Phys. Rev. B* **1999**, *59*, 1758.
(28) Heyd, J.; Scuseria, G. E.; Ernzerhof, M. *J. Chem. Phys.* **2003**, *118*, 8207.
(29) Stitzer, K. E.; Smith, M. D.; Gemmill, W. R.; zur Loye, H.-C. *J. Am. Chem. Soc.* **2002**, *124*, 13877.
(30) Kimber, S. A. J.; Senn, M. S.; Fratini, S.; Wu, H.; Hill, A. H.; Manuel, P.; Attfield, J. P.; Argyriou, D. N.; Henry, P. F. *Phys. Rev. Lett.* **2012**, *108*, 217205/1.

DOI: 10.1021/ja511745q
J. Am. Chem. Soc. 2015, 137, 636−639